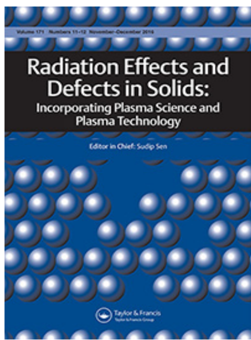

Taylor & Francis
Taylor & Francis Group

Radiation Effects and Defects in Solids
Incorporating Plasma Science and Plasma Technology

ISSN: 1042-0150 (Print) 1029-4953 (Online) Journal homepage: http://www.tandfonline.com/loi/grad20

Paschen curve approach to investigate electron density and deposition rate of Cu in magnetron sputtering system

S. Gopikishan, I. Banerjee, K. A. Bogle, A. K. Das, A. P. Pathak & S. K. Mahapatra

To cite this article: S. Gopikishan, I. Banerjee, K. A. Bogle, A. K. Das, A. P. Pathak & S. K. Mahapatra (2016) Paschen curve approach to investigate electron density and deposition rate of Cu in magnetron sputtering system, Radiation Effects and Defects in Solids, 171:11-12, 999-1005, DOI: 10.1080/10420150.2016.1267734

To link to this article: https://doi.org/10.1080/10420150.2016.1267734

Published online: 27 Dec 2016.

Submit your article to this journal

Article views: 61

View Crossmark data

Full Terms & Conditions of access and use can be found at
http://www.tandfonline.com/action/journalInformation?journalCode=grad20

RADIATION EFFECTS & DEFECTS IN SOLIDS, 2016
VOL. 171, NOS. 11–12, 999–1005
http://dx.doi.org/10.1080/10420150.2016.1267734

Taylor & Francis
Taylor & Francis Group

Paschen curve approach to investigate electron density and deposition rate of Cu in magnetron sputtering system

S. Gopikishan[a], I. Banerjee[a], K. A. Bogle[b], A. K. Das[c], A. P. Pathak[d] and S. K. Mahapatra[e]

[a]Department of Physics, Birla Institute of Technology, Ranchi, India; [b]School of Physical Sciences, Swami Ramanand Teerth Marathwada University, Nanded, India; [c]Department of Physics, Utkala University, Bhubaneswar, India; [d]School of Physics, University of Hyderabad, Hyderabad, India; [e]Centre for Physical Sciences, Central University of Punjab, Bathinda, India

ABSTRACT
In this work, Paschen curve for argon gas was obtained during copper deposition using a DC magnetron sputtering system. Five process parameters of Paschen curve were used to obtain the electron density and deposition rate of the deposited nanostructured thin films. Plasma parameter such as electron density was correlated with the deposition rate. It is observed that a minimum deposition rate was obtained for the plasma process parameter corresponding to the Paschen minimum. This investigation helps to understand and optimize the quality of nanostructured thin films depending on the process parameters.

ARTICLE HISTORY
Received 15 October 2016
Accepted 28 November 2016

KEYWORDS
Paschen curve; electron density; deposition rate; grain size

1. Introduction

Nano-particle technology plays an important role in the development of electronic devices, advanced ceramics, new batteries, engineered catalysts, biotechnology, sensors, solar cells and hydrogen storage (*1*–*5*). A DC magnetron sputtering system is commonly used to develop nanostructured thin films with unique physical, chemical, biological, mechanical and electrical properties (*6*–*9*). For certain applications, it is crucial to produce particular size-based nanostructured thin films on a large scale. One difficult issue is to optimize the process parameters to obtain the required size of the nanostructure and prevent agglomeration and control morphology in the synthesized nanostructure. As the process parameters such as voltage and pressure control the ionization rate which leads to the nucleation and growth of nanostructured thin films (*10*,*11*), the optimization of these process parameters of the DC magnetron sputtering system is still a topic of interest for many researchers toward achieving excellence in nanostructured film technology. However, only a few reports are available in the literature, but a systematic study is lacking.

In this work, Paschen curve for argon (Ar) gas was obtained during copper (Cu) deposition using the DC magnetron sputtering system. Five process parameters were chosen from the Paschen curve and used to obtain the electron density (n_e) and deposition rate (D_r) of the deposited nanostructured films. Plasma parameters such as electron density were correlated to the deposition rate.

CONTACT S. K. Mahapatra skmahapatra741973@gmail.com

© 2016 Informa UK Limited, trading as Taylor & Francis Group

2. Experimental details

The experiment performed in a DC magnetron sputtering system is shown in Figure 1. It consists of (a) a DC power supply, (b) a source meter (SM), (c) a Wilson-seal port, (d) an upper flange, (e) a cylindrical stainless steel chamber of diameter 270 mm and length 230 mm, (f) a magnetron sputter gun, (g) a Cu target of size 2″ diameter and 5 mm thickness, (h) an MFC flow meter, (i) a Langmuir probe (LP) setup (provided by the Excel Instruments Pvt. Ltd., India), (j) a vacuum pump, (k) a substrate holder and (l) a bottom flange. The upper flange carries the LP and the bottom flange carries the substrate holder. The Langmuir probe of diameter ∼0.5 mm and length 40 mm is electrically isolated and connected to the Keithley source meter. The plasma current was collected corresponding to the applied potential to the LP.

Silicon substrates of size 0.5 cm × 0.5 cm were obtained by cutting a silicon wafer and mounting them on the sample holder. The silicon substrates were cleaned using diluted hydrogen fluoride acid, ultra-sonicated with acetone for 20 minutes and dried at room temperature prior to deposition. Before deposition, the base pressure of the plasma chamber was maintained at 2×10^{-6} mbar. Then, various working pressures were obtained by adjusting the Ar gas flow rate to the plasma chamber. Initially, at a working pressure (P), the DC voltage was increased slowly to ignite the plasma, attaining the break down voltage at

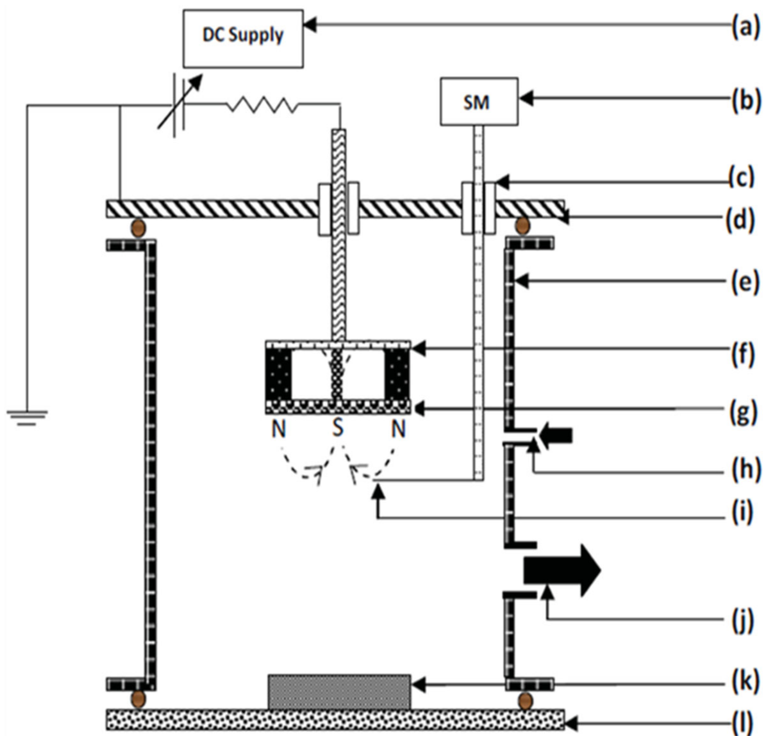

Figure 1. Schematic diagram of the DC magnetron sputtering system, (a) DC power supply, (b) source meter, (c) Wilson seal port, (d) upper flange, (e) cylindrical stainless steel chamber, (f) magnetron sputter gun, (g) Cu target, (h) MFC flow meter, (i) Langmuir probe setup, (j) vacuum pump port, (k) substrate holder and (l) bottom flange.

constant anode–cathode gap ($d = 10$ cm). Similarly, for different working pressures of Ar gas, break down voltages were measured and the Paschen curve was obtained.

Paschen curve, that is, breakdown voltage (V_b) vs. Pressure × distance (Pd), is shown in Figure 2. Five combinations of V_b and Pd were used for the measurement of electron density and deposition rate. Electron density and deposition rate were correlated with process parameters using the graph of n_e vs. Pd and D_r vs. Pd.

For the accurate measurement of electron density, a cylindrical tungsten wire commonly known as Langmuir probe (LP) was used. This probe was mounted on a quartz plate and connected to the Keithley source meter (Model No: 2410). After plasma ignition at a certain gas pressure and voltage, I–V characteristic was obtained through the LP. From the I–V plots, n_e was estimated and the n_e vs. Pd plot for ignited plasma is shown in Figure 4.

The weight of the nanostructured copper film on the silicon substrate at five different combinations of process parameters (V_b and Pd) was obtained by measuring and calculating the weight difference of the substrate before and after deposition using a digital analytical balance (Mettler Toledo, Germany). The deposition rate was estimated by dividing the weight difference of the substrate by sputtering time.

$$D_r = \frac{W_2 - W_1}{t_2 - t_1},$$

where w_2 is the weight of the silicon substrate after deposition, w_1 is the weight of the silicon substrate before deposition, t_1 is the starting time of deposition and t_2 is the ending time of deposition. Further, the grain size was estimated using an Atomic Force Microscope (model: solver Pro-47, operation mode: noncontact/tapping mode, silicon nitride tip was used, with frequency 427 kHz and scan speed 0.5 Hz).

3. Results and discussion

The Paschen curve (V_b vs. Pd) of Ar in the DC magnetron sputtering system is shown in Figure 2. It attained a minimum value of breakdown voltage (V_b) known as Paschen

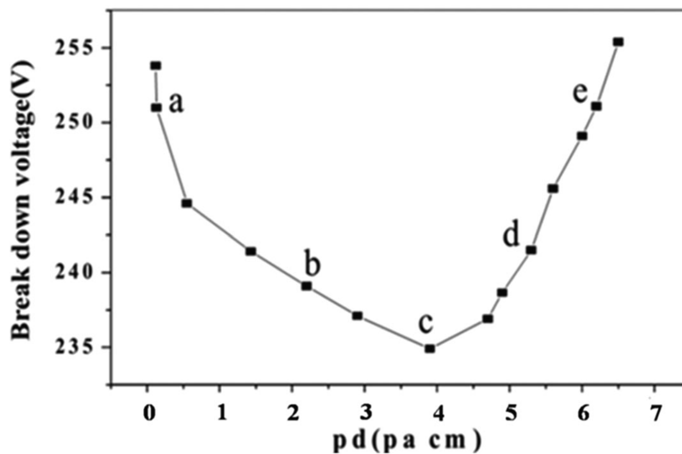

Figure 2. Paschen curve of the DC magnetron sputtering system: (a) 0.13, (b) 2.2, (c) 3.9, (d) 5.3 and (e) 6.2 Pa cm.

minimum which divides the pressure range in high voltage-low current (left-hand side (LHS) of the Paschen minimum) and low voltage-high current regime (right-hand side (RHS) of the Paschen minimum). Breakdown voltage increases on both sides of the Paschen minima corresponding to $\sim$3.9 Pa cm. This nature was expected because at the RHS of the Paschen minimum, the increased pressure zone is governed by more frequent collisions in the electron path, but this results in a reduction of electron energy which fails in the ionization of atoms. Therefore, larger voltage for electrons is required to provide sufficient energy to ionize the gas atoms and reach avalanche state. On the other hand, on the LHS of the Paschen minimum, the pressure is less; hence, the mean free path (MFP) is longer, although the electrons have more energy but accompanied by fewer collisions. Hence, again a greater breakdown voltage is required to ionize the gas atoms to start the avalanche.

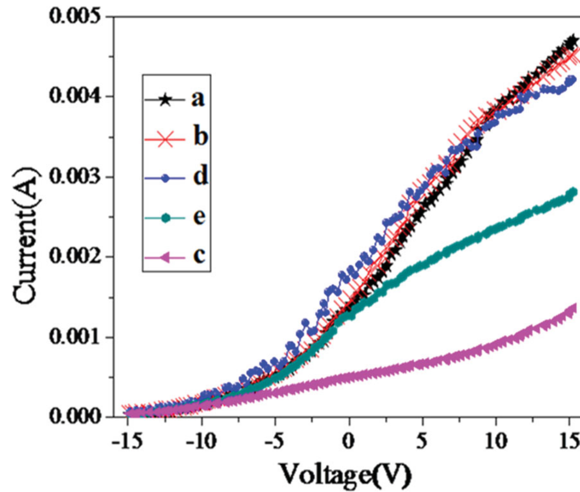

Figure 3. *I–V* plots at five different pressures: (a) 0.13, (b) 2.2, (c) 3.9, (d) 5.3 and (e) 6.2 Pa cm of the Paschen curve.

Electron density plays a major role in the energy transfer to the substrate for deposition. Figure 3 shows *I–V* plots at five different pressures: (a) 0.13, (b) 2.2, (c) 3.9, (d) 5.3 and (e) 6.2 Pa cm of the Paschen curve. The electron density was estimated using the standard relation (*12*, *13*) as

$$n_e = \frac{I_{es}}{eA\sqrt{\frac{K_B T_e}{2\pi m_e}}},$$

where I_{es} is the electron saturation region in the *I–V* plot (Figure 3), e is the electron charge, A is an area of the probe, K_B is the Boltzmann constant, T_e is the electron temperature and m_e is the electron mass.

Figure 4 shows the electron density, n_e vs. five different combinations of Pd (a) 1.3, (b) 2.2, (c) 3.9, (d) 5.3 and (e) 6.2 Pa cm. The electron density seems to follow the Paschen curve, with its minimum coinciding with the Paschen minimum.

The deposition rate (D_r) at five different combinations of Pd is shown in Figure 5. The maximum deposition rate obtained at both sides of the Paschen minimum may be due to the fact that both breakdown voltage and deposition rate are driven by electron collisions

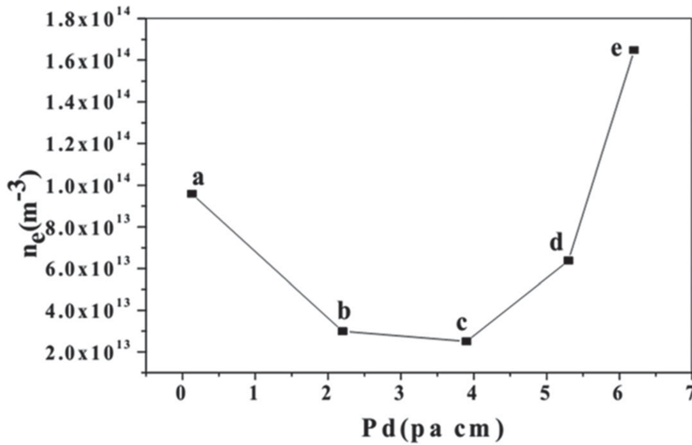

Figure 4. Electron density, n_e, at five different pressures: (a) 0.13, (b) 2.2, (c) 3.9, (d) 5.3 and (e) 6.2 Pa cm of the Paschen curve.

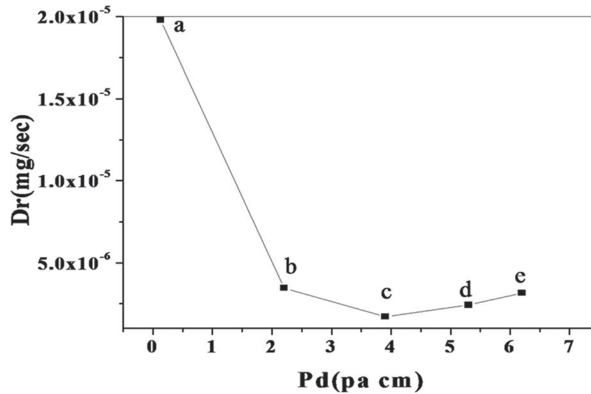

Figure 5. Deposition rate, D_r, at five different pressures: (a) 0.13, (b) 2.2, (c) 3.9, (d) 5.3 and (e) 6.2 Pa cm of the Paschen curve.

with the gas neutrals, leading to ionization, dissociation, etc. On the LHS of the Paschen minima, voltage dominates, whereas on the RHS of the Paschen minima, pressure dominates in the deposition condition. It is found that the deposition rate decreases up to the Paschen minima and then increases slowly on the RHS. This was expected because the MFP on the LHS decreases with increasing pressure, causing a relatively large number of collisions leading to a decrease in the deposition rate with an increase in pressure. On the RHS of the Paschen minima, the pressure increases further; but here the collision induced is partly compensated by electron density increase, resulting in a slow increase in the deposition rate (*14*).

The nanostructured film growth process is driven by different combinations of Pd and V_b, leading to different deposition rates through heterogeneous gas phase nucleation. However, the magnetic field in magnetron undergoes competition between the collision-induced scattering/diffusion of electrons with the gas molecules (electron MFP)

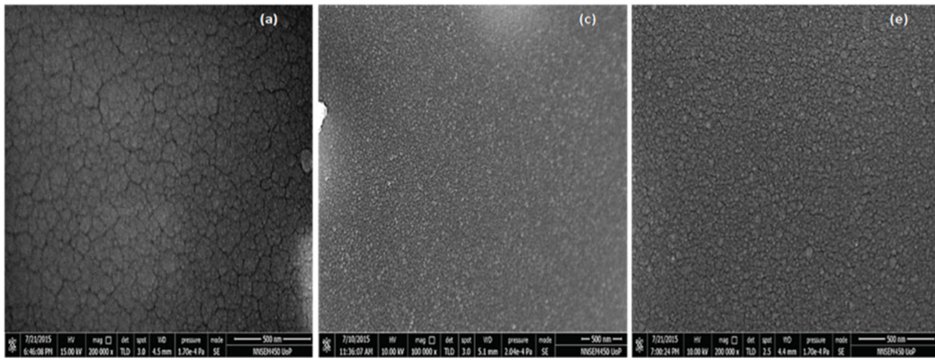

Figure 6. Typical grain size at three different pressures: (a) 0.13, (b) 3.9 and (c) 6.2 Pa cm of the Paschen curve.

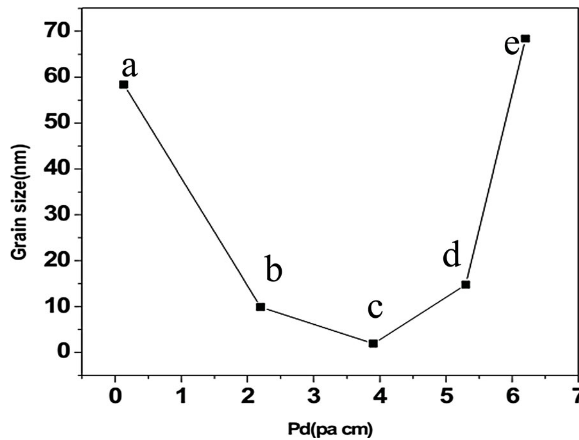

Figure 7. Grain size of thin films at five different pressures: (a) 0.13, (b) 2.2, (c) 3.9, (d) 5.3 and (e) 6.2 Pa cm of the Paschen curve.

and electron confinement within a cyclotron radius. Hence, reactive species get confined in the magnetic field and as a consequence, pure deposition with very less contamination for a longer period of time without any peeling effects of residuals and particle formation is achieved. Similar results were obtained by Ledernez et al. (*15*).

It is interesting to obtain the grain size and correlate it with the electron density, because it is well-known that the electron density becomes large enough for crystal growth at both sides of the Paschen minimum. Thus, based on the value of the electron density, the grain size can be predicted. The typical grain size for three different values of pressure (P), that is, (a) 0.13, (b) 3.9 and (c) 6.2 Pa cm, of the Paschen curve is shown in Figure 6. Grain size was evaluated using the molecular device and tools for nanotechnology (NT-MDT), NOVA is the name of software by threshold calculation of the topographical data of the given sample, and average of all the image (not given) data was used for the given sample shown in Figure 7. It shows the grain size increases on the LHS and RHS of the Paschen minimum. On the LHS of the Paschen minimum, as shown in Figure 2, the MFP of the electrons is longer and the electrons undergo less collision, which provides more time for grain growth. This may lead

to an increase in the grain size which decreases with an increase in pressure till reaching the Paschen minimum. However, the RHS of the Paschen minimum (Figure 2) is governed by less efficient collision-based reactions due to very small MFP of electrons. This further causes larger clustering and agglomeration, hence the grain size increases. The density and size of the nanostructured film critically depend on the collision and mobility of the moving atomic species. Therefore, this method of Paschen curve minima can be utilized for the deposition of the nanostructured thin films with quantitative control of thickness and grain size.

4. Conclusion

A DC magnetron sputtering system was designed and characterized with the help of the Paschen curve. It was observed that the deposition rate could be controlled through the Paschen curve analysis. The minimum deposition of smallest grain size can be observed at the Paschen minimum and maximum on both sides of the Paschen minima. This could help in optimizing the plasma parameters to develop the required coating for the modern technology.

Acknowledgement

APP would like to thank CSIR, New Delhi for the Emeritus Scientist award.

Disclosure statement

No potential conflict of interest was reported by the authors.

Funding

The authors gratefully acknowledge the financial support of the Science and Engineering Research Board (SERB), Department of Science and Technology (DST), Government of India (Ref No: EMR/2014/000722).

References

(1) Shi, J.Z.; Chen, C.Z.; Yu, H.J.; Zhang, S.J. *Bull. Mater.Sci.* **2008,** *31,* 877–884.
(2) Groenen, R.; Linden, J.L.; Van Lierop, H.R.; Schram, D.C.; Kuypers, A.D.; Van De Sanden, M.C. *Appl. Surf.Sci.* **2001,** *173,* 40–43.
(3) Park, K.H.; Dhayal, M. *Electrochem.Commun.* **2009,** *11,* 75–79.
(4) Hotovy, I.; Rehacek, V.; Siciliano, P.; Capone, S.; Spiess, L. *Thin Solid Films* **2002,** *418,* 9–15.
(5) Benard, W.L.; Kahn, H.; Heuer, A.H.; Huff, M.A*J.Microelectromech. Systems* **1998,** *7,* 245–251.
(6) Bender, M.; Seelig, W.; Daube, C.; Frankenberger, H.; Ocker, B.; Stollenwerk, J. *Thin Solid Films* **1998,** *326,* 72–77.
(7) Akbarnejad, E.; Ghorannevis, Z.; Ghoranneviss, M.; Elahi, A.S. *Radiat.Eff.Def. Solids* **2015,** *170,* 541–547.
(8) Ajenifuja, E.; YisauFasasi, A.; Ayo Osinkolu, G.*Trans. Indian Ceram.Soc.* **2012,** *71,* 181–188.
(9) Dejam, L.; Elahi, S.M. *Mol. Crystals Liq. Crystals* **2013,** *577,* 59–70.
(10) Hellgren, N.; Macák, K.; Broitman, E.; Johansson, M.P.; Hultman, L.; Sundgren, J.E. *J.Appl.Phys.* **2000,** *88,* 524–532.
(11) Ellmer, K.; Cebulla, R.; Wendt, R. *Thin Solid Films* **1998,** *317,* 413–416.
(12) Merlino Robert, L. *Amer. J.Phys.* **2007,** *75,* 1078–1085.
(13) Amemiya, H. *J.Phys. D: Appl.Phys.* **1990,** *23,* 999.
(14) Shah, H.N.; Chawla, V.; Jayaganthan, R.; Kaur, D. *Bull.Mater.Sci.* **2010,** *33,* 103–110.
(15) Ledernez, L.; Olcaytug, F.; Urban, G. *Contrib. Plasma Phys.* **2012,** *52,* 283–288.